

Data-Driven Estimation of Vinnicombe metric

Margarita A. Guerrero, Henrik Sandberg, and Cristian R. Rojas

Abstract—Quantifying model mismatch in a control-relevant manner is fundamental in robust control. A well-known metric for this purpose is the ν -gap, or Vinnicombe metric, which measures the discrepancy between a nominal model and the real system from a closed-loop viewpoint. However, its computation typically requires explicit knowledge of the true system. In this letter, we propose an identification-free, data-driven method to estimate the ν -gap between discrete-time SISO systems directly from input-output experiments. The method is complemented by a data-driven winding-number test, based on Welch-type averaging, to verify a required topological condition for the computation of the metric. Numerical simulations on heavy-duty gas-turbine models and a textbook example show that the proposed estimate closely matches MATLAB[®] `gapmetric`, while correctly detecting cases in which the admissibility conditions fail.

Index Terms—Data-driven modeling, System identification, Robust control.

I. INTRODUCTION

A core aim of automatic control is to design robust controllers that operate reliably despite modeling errors. In this context, robustness means that performance does not deteriorate significantly when the real system differs from the model used for the controller synthesis. Several frameworks have been developed to address this problem, including small-gain arguments [1], integral quadratic constraints (IQCs) [2], and \mathcal{H}_∞ control [3]. Essentially, these approaches provide stability or performance guarantees for all plants whose uncertainty satisfies a prescribed description, such as norm bounds, structural assumptions, or multiplier-based conditions.

A control-relevant way to quantify model mismatch is provided by the Vinnicombe metric [4, 5], also known as the ν -gap metric, defined for linear time-invariant systems (LTI). This metric is particularly appealing because it measures discrepancies between plants from a closed-loop viewpoint and induces the weakest topology in which closed-loop stability is a robust property. Thus, if the ν -gap between a nominal model and the true plant is sufficiently small, then a controller that robustly stabilizes the nominal model will also stabilize the true plant, under suitable admissibility conditions. Moreover, while topologically equivalent to the

gap metric [6, 7], the ν -gap admits a direct frequency-response interpretation.

In practice, however, the usefulness of both robust-control guarantees and ν -gap-based reasoning depends on how accurately the plant uncertainty or model mismatch can be characterized. When the true plant is unknown and prior knowledge is inaccurate, constructing a meaningful uncertainty description may be difficult, conservative, or infeasible.

This practical difficulty has motivated research on estimating control-relevant robustness quantities directly from data, in settings where only input-output measurements are available and no explicit plant knowledge is assumed [8, 9]. One prominent line of work estimates the \mathcal{H}_∞ norm of the modeling error directly from experiments by means of iterative procedures, such as power iterations [10, 11] and Thompson sampling [12]. More recently, a power-iteration-based approach for estimating the structured singular value has been proposed in [13].

To the best of our knowledge, there is no data-driven method for estimating the Vinnicombe metric. Motivated by this, we propose an identification-free, iterative approach that estimates the ν -gap between two plants directly from time-domain input-output data. The proposed method builds on the core idea of power iterations to compute a numerical estimate of the distance between two dynamical systems, while an iterative winding-number calculation is used to verify the admissibility conditions under which the ν -gap is well defined.

Our main contributions are as follows:

- We propose a novel identification-free, data-driven method for estimating the Vinnicombe metric directly from time-domain input-output experiments.
- We introduce an identification-free procedure for verifying the admissibility conditions of the ν -gap through an iterative winding-number computation based on Welch-inspired frequency-domain estimates.
- We demonstrate the effectiveness of the proposed method through numerical simulations, showing that the resulting estimates closely agree with MATLAB[®] `gapmetric`.
- We illustrate the practical applicability of the proposed framework to General Electric heavy-duty gas turbines, showing how the Vinnicombe metric can be interpreted and implemented in an industrial setting.

The remainder of this paper is organized as follows: In Section II, we state our problem setup. Section III reviews the Vinnicombe metric and the power iteration method. In Section IV, we outline our proposed approach, and demonstrate its efficacy in Section V. The paper is concluded in

This work was partly supported by the Swedish Research Council under contract number 2023-05170, by the Wallenberg AI, Autonomous Systems and Software Program (WASP), and by the Swedish Civil Defence and Resilience Agency (Project MAD-VAMCHS). The authors are with the Division of Decision and Control Systems, KTH Royal Institute of Technology, 100 44 Stockholm, Sweden (e-mails: mags3@kth.se, hsan@kth.se, crr@kth.se).

Code available at <https://github.com/mags-ono/nu-gap>.

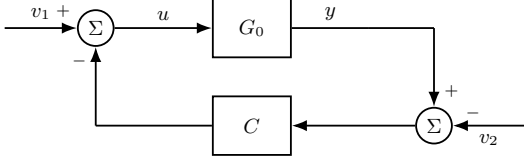


Fig. 1: Standard feedback configuration.

Section VI.

II. PROBLEM STATEMENT

Consider a stable unity-feedback interconnection of a nominal plant G_0 with a controller C , denoted by $[G_0, C]$. Suppose that the nominal plant differs from an unknown true system G . Our objective is to guarantee that the controller C will perform as intended on the true process regardless of the unmodeled dynamics. Throughout the paper, (G_0, G, C) are discrete-time, linear time-invariant, single-input single-output systems.

The aforementioned problem can be handled with a well-known distance metric, namely the ν -gap, also called the Vinnicombe metric [4, 5]. The Vinnicombe metric, denoted by δ_ν , is an appropriate measure for assessing how two systems differ in their closed-loop behavior, satisfying $0 \leq \delta_\nu(G_1, G_2) \leq 1$ (see Section III-A).

This quantity admits a closed-loop interpretation: it measures, in a normalized worst-case sense, the discrepancy between the complementary sensitivity behaviors induced by unity feedback around G and G_0 . In particular, taking a sufficiently small value of δ_ν implies that any controller that stabilizes G_0 with adequate margin also stabilizes G (under additional conditions summarized in Section III-A).

When the real plant is unknown, computing $\delta_\nu(G, G_0)$ becomes untenable, as it requires knowledge of the true process. A classical workaround is to postulate that G lies in a neighborhood of the nominal model, i.e., $\mathcal{B}_\tau(G_0) := \{\tilde{G} : \delta_\nu(\tilde{G}, G_0) \leq \tau\}$ [5, Proposition 1.2]. However, specifying such a set typically relies on prior modeling knowledge about unmodeled dynamics and may be conservative or inaccurate.

Motivated by these limitations, we propose in Section IV an identification-free, data-driven procedure to compute the Vinnicombe metric for the single-input single-output (SISO) case using a power-iteration principle [14], requiring only input-output experiments on the black-box system G and an iterative redesign of the excitation signal. While we primarily assume that G_0 is an available nominal model, the same methodology can be used as a data-driven similarity test when both systems are unknown, e.g., to compare the opening/closing dynamics of two valves from closed-loop measurements.

Before presenting the proposed approach, we introduce the technical preliminaries required throughout the manuscript.

III. PRELIMINARIES

A. The Vinnicombe Metric

Consider the standard negative-feedback interconnection of a nominal discrete-time LTI multi-input multi-output

(MIMO) plant $G_0(z)$ and a compensator $C(z)$ as shown in Fig. 1. Let v_1 and v_2 denote additive disturbances at the controller input and output, respectively, and let (y, u) be the plant output and input. The closed-loop transfer matrix from $[v_1 \ v_2]^T$ to $[y \ u]^T$ is

$$T(G_0, C) := \begin{bmatrix} G_0 \\ I \end{bmatrix} (I + CG_0)^{-1} \begin{bmatrix} -C & I \end{bmatrix}, \quad (1)$$

where $I = 1$ is the SISO case.

We define the *stability margin* of the feedback interconnection $[G_0, C]$ as

$$b_{G_0, C} := \begin{cases} \|T(G_0, C)\|_\infty^{-1}, & \text{if } [G_0, C] \text{ is stable,} \\ 0, & \text{otherwise.} \end{cases} \quad (2)$$

The number $b_{G_0, C}$ can be regarded as a measure of the performance of the feedback system comprising G_0 and C , with larger values of (2) corresponding to better performance. Note that (2) lies in the range $[0, 1]$ [4].

Definition 1: Let $G_0(z)$ and $G(z)$ be discrete-time single-input single-output (SISO) transfer functions. The Vinnicombe metric (or ν -gap) [5] between G_0 and G is defined as

$$\delta_\nu(G_0, G) = \begin{cases} \left\| \left\| \frac{G_0 - G}{\sqrt{(1 + |G_0|^2)(1 + |G|^2)}} \right\| \right\|_\infty, & \text{if } (G_0, G) \in \mathcal{C}, \\ 1, & \text{otherwise.} \end{cases} \quad (3)$$

where $(G_0, G) \in \mathcal{C}$ if the functions $f_1(z) := 1 + G_0(z)G_0(z^{-1})$ and $f_2(z) := 1 + G(z)G_0(z^{-1})$ have the same number of zeros in $\mathbb{E} := \{z \in \mathbb{C} : |z| > 1\}$.

The condition $(G_0, G) \in \mathcal{C}$ is an index (winding-number) requirement that ensures a meaningful notion of continuity: if G is perturbed continuously away from G_0 , it rules out situations in which an intermediate plant \tilde{G} would necessarily yield $\delta_\nu(\tilde{G}, G_0) = 1$ even though $\delta_\nu(G, G_0)$ is small [15, Section 12.1]. In the SISO case, this condition can be checked via a Nyquist/winding-number test, where the winding number is denoted by $\text{wno}(\cdot)$; in particular, the Nyquist plot of $G(e^{j\omega})G_0(e^{-j\omega})$ should not encircle the critical point -1 for $\omega \in (-\pi, \pi]$. Additionally, in this same SISO setting, the pointwise quantity underlying the ν -gap admits a geometric interpretation as the chordal distance between the projected Nyquist diagrams of two plants onto the Riemann sphere [5, Sec. 3]. Therefore, δ_ν may be viewed as the maximum normalized separation over frequency, which explains its relevance as a closed-loop similarity metric.

Proposition 1 ([5, Prop. 1.2]): Given a nominal plant G_0 and a perturbed plant G , the interconnection $[G, C]$ is stable for all compensators C satisfying $b_{G_0, C} > \beta$ if and only if $\delta_\nu(G_0, G) \leq \beta$.

The ν -gap metric $\delta_\nu(G_0, G)$ quantifies the distance between two plants from a closed-loop perspective. In particular, $\delta_\nu(G_0, G) \in [0, 1]$, with $\delta_\nu(G_0, G) = 0$ if and only if $G_0 = G$. Hence, when G represents the (unknown) true plant, a small value of $\delta_\nu(G_0, G)$ indicates that the mismatch

between G_0 and G is negligible in terms of closed-loop stability.

B. Power Iteration Method

In order to compute (3), one needs to compute the \mathcal{H}_∞ norm of a transfer function. To this end, consider a linear discrete-time stable causal and proper system of the form

$$y_k = G(q)u_k + e_k$$

where $\{u_k\}$ is an input signal, G is a transfer function, $\{y_k\}$ is the output of the system, and $\{e_k\}$ is Gaussian, not necessarily white noise. Next, recall that the \mathcal{H}_∞ norm is an induced norm, i.e., $\|G\|_\infty = \|G\|_{i2}$; see [?, App. A.5.7] for a proof. Assume that, at iteration t , the signals have a finite length $N \in \mathbb{N}$, i.e., $\mathbf{u}^t := [u_0^t, \dots, u_{N-1}^t]^T$, $\mathbf{y}^t := [y_0^t, \dots, y_{N-1}^t]^T \in \mathbb{R}^{N \times 1}$, hence

$$\|G\|_{i2,N} = \sup_{\mathbf{u}^t \in \mathbb{R}^{N \times 1} \setminus \{0\}} \frac{\|\mathbf{y}^t\|_2}{\|\mathbf{u}^t\|_2}, \quad (4)$$

where $\|G\|_{i2,N} \rightarrow \|G\|_\infty$ for $N \rightarrow \infty$ [11, Th. 3]. Let us assume that, at iteration t , the system starts from zero initial conditions. If there is no noise affecting the output of the system, the mapping from \mathbf{u}^t to \mathbf{y}^t can be written as

$$\mathbf{y}^t = \mathbf{G}_N \mathbf{u}^t,$$

where

$$\mathbf{G}_N = \begin{bmatrix} g_0 & 0 & 0 & \cdots & 0 \\ g_1 & g_0 & 0 & \cdots & 0 \\ \vdots & \ddots & \ddots & \ddots & \vdots \\ g_{N-1} & g_{N-2} & \cdots & g_1 & g_0 \end{bmatrix}$$

is a triangular Toeplitz matrix. Thus, (4) is equivalent to

$$\|G\|_{i2,N}^2 \approx \sup_{\mathbf{u}^t \neq 0} \frac{(\mathbf{u}^t)^T \mathbf{G}_N^T \mathbf{G}_N \mathbf{u}^t}{(\mathbf{u}^t)^T \mathbf{u}^t} = \lambda^{\max}(\mathbf{G}_N^T \mathbf{G}_N). \quad (5)$$

The right hand side, known as the *Rayleigh quotient* of $\mathbf{G}^T \mathbf{G}$, corresponds to the largest eigenvalue of $\mathbf{G}^T \mathbf{G}$, and it can be computed using the power iteration method.

Procedure 1 (Power Iteration Method): Consider a square matrix $\mathbf{A} \in \mathbb{R}^{n \times n}$. The power iteration method performs the following steps to estimate the eigenvector of \mathbf{A} corresponding to its largest eigenvalue:

1. Choose $\mathbf{x}_0 \in \mathbb{R}^n$ randomly.
2. Set $i \leftarrow 1$.
3. Compute $\mathbf{x}_i \leftarrow \frac{1}{\|\mathbf{A}\mathbf{x}_{i-1}\|_2} \mathbf{A}\mathbf{x}_{i-1}$.
4. Set $i \leftarrow i + 1$ and go to Step 3.

For normalized iterates, a natural estimate of the magnitude of the dominant eigenvalue is $\|\mathbf{A}\mathbf{x}_{i-1}\|_2^1$.

In the SISO frequency-domain setting, the \mathcal{H}_∞ norm coincides with the maximum magnitude of the frequency response over all frequencies, i.e., with the peak of the Bode magnitude plot. Thus, the same power-iteration principle can be interpreted in the frequency domain as an iterative search for the peak gain, where the maximizing frequency is implicitly identified by the iterations.

¹If \mathbf{A} is symmetric, the dominant eigenvalue may also be estimated through the Rayleigh quotient $\mathbf{x}_{i-1}^T \mathbf{A} \mathbf{x}_{i-1}$. The two estimates may differ numerically under noise or finite-iteration effects.

Our proposed procedure retains this template to approximate the ν -gap in (3) based solely on experiments on the unknown system G . We assume $e_k = 0$ throughout the analysis, while noise is included in the simulations of Section V to evaluate robustness.

IV. PROPOSED APPROACH

In this section, we propose a data-driven procedure to estimate the Vinnicombe ν -gap metric from time-domain experiments. Assuming that a nominal model G_0 is available and that only input-output data can be collected, we adapt the model-based construction in [4] to operate directly on frequency-domain quantities estimated from time-domain data.

Data-gap estimation
We focus on the practically relevant setting where G denotes the (unknown) plant and G_0 is a nominal model. For a given input u , let $U(e^{j\omega})$ be its discrete-time Fourier transform (DFT), and let $Y(e^{j\omega})$ and $Y_0(e^{j\omega})$ denote the corresponding output spectra obtained from experiments on G and G_0 , respectively, so that $Y(e^{j\omega}) = G(e^{j\omega})U(e^{j\omega})$ and $Y_0(e^{j\omega}) = G_0(e^{j\omega})U(e^{j\omega})$. When $(G, G_0) \in \mathcal{C}$, the ν -gap admits the equivalent frequency-domain expression

$$\delta_\nu(G, G_0) = \sup_{\omega \in (-\pi, \pi]} \frac{|U(e^{j\omega})|^2 |Y(e^{j\omega}) - Y_0(e^{j\omega})|}{\sqrt{|U(e^{j\omega})|^2 + |Y(e^{j\omega})|^2} \sqrt{|U(e^{j\omega})|^2 + |Y_0(e^{j\omega})|^2}}.$$

As in \mathcal{H}_∞ norm estimation, the ν -gap is the supremum of the modulus of a frequency function. In the noiseless case, this motivates a power-iteration-type input redesign that progressively concentrates excitation at frequencies that dominate the above ratio. Specifically, given spectra (U^n, Y^n, Y_0^n) at iteration n , we update the next input in the frequency domain according to

$$\tilde{U}^{n+1}(e^{j\omega}) = \frac{|U^n(e^{j\omega})|^2 [Y^n(e^{j\omega}) - Y_0^n(e^{j\omega})]}{\sqrt{|U^n(e^{j\omega})|^2 + |Y^n(e^{j\omega})|^2} \sqrt{|U^n(e^{j\omega})|^2 + |Y_0^n(e^{j\omega})|^2}} \quad (6)$$

The role of (6) is then analogous to that of the matrix-vector product in the classical power iteration: each update amplifies the frequency components that contribute most to the normalized discrepancy between G and G_0 . The updated spectrum is mapped back to the time domain via an inverse DFT, normalized, and used in the next experiment. Thus, the input progressively concentrates near the frequency at which the ν -gap is attained.

B. wno estimation

The update rule in (6) suggests a straightforward implementation; however, the index condition $(G_0, G) \in \mathcal{C}$ cannot be overlooked. This condition rules out pathological situations where, despite a small closed-loop mismatch between G_0 and G , any continuous path from G_0 to G would necessarily cross an intermediate transfer function \tilde{G} for which the ν -gap saturates to one. Accordingly, we verify that $(G_0, G) \in \mathcal{C}$ in a data-driven fashion by computing winding numbers of the index functions f_1 and f_2 , i.e., by checking

that the Nyquist curve of $G(e^{j\omega})G_0(e^{-j\omega})$ does not encircle the critical point -1 for $\omega \in (-\pi, \pi]$.

Using the same information from the Fourier transform of the input and outputs of (6), and inspired by Welch's method [16] we compute f_2 as follows:

$$f_2(e^{j\omega_k}) \approx \frac{1 + \frac{\left(\sum_{n=1}^{N_{\text{acc}}} Y_n[k] U_n[k]^*\right) \left(\sum_{n=1}^{N_{\text{acc}}} Y_{0,n}[k] U_n[k]^*\right)^*}{\left(\max\left(\sum_{n=1}^{N_{\text{acc}}} |U_n[k]|^2, \varepsilon_0\right)\right)^2}, \quad (7)$$

where n is the current iteration, $\omega_k := 2\pi k/N$, $k \in \{0, 1, \dots, N-1\}$ is the DFT grid on the unit circle, N_{acc} is the number of iterations used to approximate f_2 , and ε_0 is a small number to avoid division by 0. An analogous expression can be written for f_1 by replacing $(Y_n, Y_{0,n})$ with $(Y_{0,n}, Y_{0,n})$ in (7). Inspired by Welch's averaged periodogram estimator [17, Ch. 6, Eq. (6.70)], we estimate the index functions by averaging across power-iteration experiments. Unlike classical Welch's method, which partitions a single record into multiple sub-batches and recomputes the DFT for each batch, our approach reuses the DFTs that are already computed at each power-iteration step. We therefore average over the first $N_{\text{acc}} \ll M$ iterations: as the power method progresses, the redesigned input becomes increasingly narrowband around the peak frequency, which reduces spectral coverage and makes later iterations less informative for index verification [11]. Finally, for $i \in \{1, 2\}$, let $f_i[k] := f_i(e^{j\omega_k})$ denote the samples of f_i on the DFT grid. We compute the winding numbers $\text{wno}(f_2)$ and $\text{wno}(f_1)$ by summing discrete phase increments of f_i around the unit circle, where we set $f_i[N] := f_i[0]$ to close the sampled path. Specifically, we define

$$\Theta_i = \sum_{k=0}^{N-1} \arg\left(\frac{f_i[k+1]}{f_i[k]}\right), \quad \text{wno}(f_i) = \text{round}\left(\frac{\Theta_i}{2\pi}\right). \quad (8)$$

The data-driven winding-number computation is summarized in Algorithm 2.

These considerations lead to the pseudo-code for the data-driven computation of the Vinnicombe metric in Algorithm 1. The procedure terminates early if $\text{wno}(f_1) \neq \text{wno}(f_2)$ within the first N_{acc} iterations (indicating $(G_0, G) \notin \mathcal{C}$); otherwise, it runs for the full M iterations.

V. EXPERIMENTS

This section presents simulation studies to assess Algorithms 1–2. The study includes: (i) two heavy-duty gas-turbine case studies, where ν -gap estimates are benchmarked against MATLAB's `gapmetric`; and (ii) a synthetic/textbook example for which the winding number condition is analytically verifiable.

A. Case Study: Heavy-Duty Gas Turbine

Heavy-duty gas turbines (HDGTs) are large industrial gas turbines used mainly for power generation. They consist of an axial-flow compressor, combustor chambers where fuel is burned, and a turbine section that expands the hot

Algorithm 1 Data-driven estimation of the ν -gap

Require: A random input vector $\mathbf{u}^0 \in \mathbb{R}^N$

- 1: **for** $n = 0, 1, 2, \dots, M-1$ **do**
 - 2: Apply \mathbf{u}^n to G and G_0 , and collect outputs \mathbf{y}^n and \mathbf{y}_0^n , respectively.
 - 3: Compute the DFT of \mathbf{u}^n , \mathbf{y}^n and \mathbf{y}_0^n , and calculate (6), for each frequency ω .
 - 4: **if** $n < N_{\text{acc}}$, update accumulators via
 $S_{yu} += Y_n[k]U_n[k]^*$, $S_{y_0u} += Y_{0,n}[k]U_n[k]^*$, $S_u += |U_n[k]|^2$
end if
 - 5: **if** $n = N_{\text{acc}}$ **then**
 - 6: **Run** Algorithm 2
 - 7: **if** `inC` is false, **Terminate** and set $\delta_\nu \leftarrow 1$ **end if**
 - 8: **end if**
 - 9: Compute $\tilde{\mathbf{u}}^{n+1}$ as the IDFT of $\tilde{U}^{n+1}(e^{j\omega})$
 - 10: Normalize $\tilde{\mathbf{u}}^{n+1}$ by its 2-norm to obtain \mathbf{u}^{n+1}
 - 11: **end for**
 - 12: Estimate δ_ν as the 2-norm of $\tilde{\mathbf{u}}^M$
-

Algorithm 2 Data-driven index condition $(G_1, G_2) \in \mathcal{C}$

Require: Accumulators (S_{yu}, S_{y_0u}, S_u) , N_{acc} batches; tolerance $\varepsilon_0 > 0$; threshold $\text{tol}_f > 0$.

- 1: **for** $n = 0, 1, \dots, N_{\text{acc}}$, Construct f_1 and f_2 via (7), **end for**
 - 2: Compute minimum distances to the origin: $m_1 = \min_k |f_1[k]|$ and $m_2 = \min_k |f_2[k]|$.
 - 3: Compute winding numbers via (8), with $f_i[N] = f_i[0]$, $i \in \{1, 2\}$
 - 4: Set `inC` $\leftarrow (m_1 > \text{tol}_f) \wedge (m_2 > \text{tol}_f) \wedge (\text{wno}(f_1) = \text{wno}(f_2))$
-

gases to produce shaft work, typically driving an electrical generator. A key control variable is the Gas Control Valve (GCV), which regulates the fuel flow into the combustor and therefore directly affects the generated power. In this work, we adopt the well-known Rowen representation for heavy-duty gas turbines [18] and consider a reduced input-output model from the (measured) GCV position u_{GCV} to generated power P , obtained by cascading: (i) a fuel dynamics $G_{f,\text{cl}}$, (ii) a combustor delay, (iii) a compressor-discharge dynamics G_{cd} , and (iv) the fuel-to-torque (power) map F_2 .

Specifically, the fuel-path dynamics $W_f(s)$ are modeled as

$$W_f(s) = G_{cd}(s) e^{-sT_{CR}} G_{f,\text{cl}}(s) u_{\text{GCV}}(s),$$

with

$$G_{f,\text{cl}}(s) = \frac{1}{T_f s + 1 + K_F}, \quad G_{cd}(s) = \frac{1}{T_{cd} s + 1},$$

where T_f is the fuel-system time constant, K_F the fuel-system feedback gain, T_{CR} the combustion reaction time delay, and T_{cd} the compressor-discharge time constant.

The (affine) torque/power map is given by

$$P = F_2(W_f, N) = A + B W_f + C(1 - S), \quad (9)$$

where S is the per-unit rotor speed and $\{A, B, C\}$ are Rowen torque-block parameters.

For grid-connected operation, speed deviations are small and we take $S \approx 1$ over the considered operating windows. Linearizing (9) around an operating point and using incremental signals (denoted by $\Delta(\cdot)$) yields the LTI incremental plant

$$G(s) := \frac{\Delta P(s)}{\Delta u_{\text{GCV}}(s)} = \frac{B e^{-sT_{CR}}}{(T_f s + 1 + K_F)(T_{cd} s + 1)}. \quad (10)$$

A.1. Nominal Model

In [19], the parameters of Rowen’s model for HDGT are estimated for a 172-MW simple cycle, single shaft power unit by using operational data at a nominal point. Following the setup in Section II, we treat the parameter values in [19, Table VII] as the closest available description of the true plant G .

Next, we assume that a nominal transfer function G_0 from the (measured) GCV position u_{GCV} to generated power P has been identified by means of a multi-objective differential evolution optimization algorithm as described in [20]. The parameters in [20, Table II], are estimated based on real data acquired from a gas turbine of 162 MW nominal power.

Assume that we have derived a controller C that stabilizes G_0 on a high-fidelity industrial simulator. The objective is to assess whether deploying C on the true operating power station is justified from a closed-loop robustness viewpoint, by estimating $\delta_\nu(G_0, G)$ from data. To emulate realistic operating constraints, we consider that the plant is under *dispatch* instructions², so that only small variations in generated power are permitted during testing. Under these constraints, we apply a bounded excitation signal $\mathbf{u}^0 \in \mathbb{R}^N$ (small-signal variations around the operating point) to both G and G_0 , collect the corresponding input-output data, and run Algorithm 1 to obtain a data-driven estimate of the ν -gap and the associated index-condition check.

As shown in Fig. 2, the Monte Carlo (MC) average of the proposed estimate $\hat{\delta}_\nu$, computed over 100 runs, becomes nearly settled after roughly 60 iterations and approaches MATLAB’s reference value $\delta_\nu = 0.2172$, indicating convergence of the proposed power-iteration scheme. The estimate is computed using $N_{\text{acc}} = 10$, $N = 9000$, $T_s = 0.05$, and measurement-noise variance $\sigma_y^2 = 0.01$ on both plants.

To further interpret this result, we inspect the dominant frequency in the last iteration and estimate the nominal local gain as $p_0(\omega_{\text{peak}}) \approx \frac{Y_0(\omega_{\text{peak}})}{U(\omega_{\text{peak}})}$, where Y_0 and U are the DFTs of the nominal output and input, respectively. In this case, the dominant peak occurs at $\omega_{\text{peak}} \approx 0.136$ rad/sample, with $|p_0(\omega_{\text{peak}})| \approx 0.54$. According to Vinnicombe’s Riemann-sphere interpretation [5, Section 3], a ν -gap around 0.2 corresponds to a relatively small discrepancy near unity gain, namely, at frequencies where $|p_0(\omega)| \approx 1$. In the present case, however, the maximizing frequency lies below unity gain, since $|p_0(\omega_{\text{peak}})| \approx 0.54$. Still, the value $\hat{\delta}_\nu = 0.2172$ suggests that the nominal and real plants are reasonably close from a closed-loop viewpoint. In particular, if the deployed controller C satisfies $b_{G_0, C} > 0.2172$, then Proposition 1 guarantees that it also stabilizes the true plant.

A.2. Unknown Models

Rowen’s model provides simplified dynamic representations for a broad range of General Electric (GE) heavy-duty, single-shaft gas turbines and accommodates both liquid- and gas-fuel systems. In particular, GE’s Frame 6F and

²In power systems, “dispatch” refers to grid-operator instructions on power setpoints and allowable load variations.

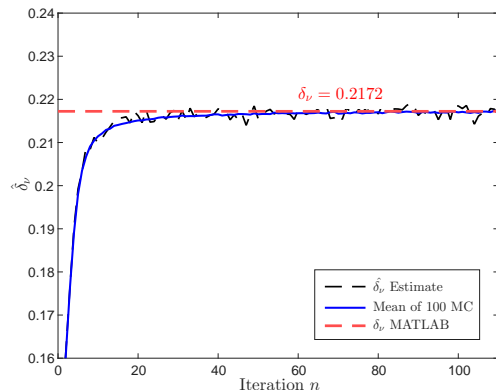


Fig. 2: Estimate of the ν -gap $\hat{\delta}_\nu$ (black, dashed), average of 100 Monte Carlo (MC) simulations (blue, solid), and actual δ_ν (red, dashed).

Frame 9F are representative mid- and high-power units (approximately 88 MW and 294 MW, respectively) for which Rowen reports “simplified” parameter sets and associated fuel/dynamic characteristics; see [18, Notes 4-7]. With the rapid growth of weather-dependent solar and wind generation, gas-fired power plants are increasingly required to provide renewable-balancing services, making operational flexibility a critical requirement. GE’s Dry Low NO_x (DLN) combustor systems [21], including recent F-class upgrades such as the DLN2.6+ platform [22], support such flexible operation while meeting tightening emissions regulations. Maintaining this performance, however, typically requires periodic tuning by a technical advisor (TA), often through on-site campaigns lasting 1–3 days depending on the scope. For Frame 6F/9F units, tuning the gas control valves (GCVs) is central to DLN performance, since these valves regulate the fuel flow and, together with other actuators, determine the combustor operating condition, emissions, and load response.

We consider a natural-gas power station equipped with both a Frame 9F and a Frame 6F unit (not necessarily within the same train). Suppose the 9F unit has been successfully tuned to comply with NO_x constraints, and the operator aims to achieve comparable emissions compliance on the 6F unit. In practice, however, limited TA availability and dispatch constraints may prevent executing a full emissions test campaign for the DLN2.6+ procedure. As a result, the plant seeks an alternative, low-impact procedure to assess whether the existing GCV tuning/controller settings developed for the 9F are compatible with the 6F, while remaining within allowable small power variations approved by dispatch.

Let $G_1(z)$ and $G_2(z)$ denote the (unknown) discrete-time transfer functions from the GCV input u_{GCV} to generated power P for the 9F and 6F units, respectively. By applying Algorithm 1 to short, bounded tests on each unit, the maintenance team can obtain a data-driven estimate of the ν -gap between G_1 and G_2 and thus quantify the degree of closed-loop mismatch. This enables an assessment of whether a GCV controller that stabilizes G_1 is likely to deliver comparable performance on G_2 , i.e., whether the plant-to-plant mismatch is sufficiently small for safe deployment. Using the parameter sets in [18, Notes 4-7], we proceed to estimate

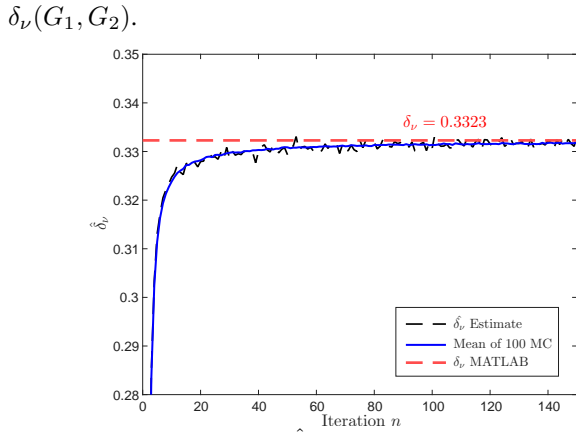


Fig. 3: Estimate of the ν -gap $\hat{\delta}_\nu$ (black, dashed), average of 100 MC simulations (blue, solid), and actual δ_ν (red, dashed).

Using the same parameters as before ($N_{\text{acc}} = 10$, $N = 9000$, $T_s = 0.05$, and $\sigma_y^2 = 0.01$), the MC mean of the proposed estimate over 100 runs stabilizes after about 100 iterations and converges in Fig. 3 to MATLAB’s value $\delta_\nu = 0.3323$. The dominant peak is attained at $\omega_{\text{peak}} \approx 0.0126$ rad/sample, with $|p_0(\omega_{\text{peak}})| \approx 0.644$, which places the maximizing frequency closer to nominal unity gain. From Vinnicombe’s Riemann-sphere interpretation, this makes the geometric intuition behind the ν -gap more directly relevant here; nevertheless, the larger value $\hat{\delta}_\nu = 0.3323$ still indicates a non-negligible degree of closed-loop similarity. From a practical viewpoint, this suggests that a controller tuned for the GE 9F unit may also be applicable to the GE 6F unit. A formal guarantee, however, would require estimating the corresponding stability margin $b_{G_{9F}, C}$, for example through a power-iteration-based estimate of $\|T(G_{9F}, C)\|_\infty$. In that case, Proposition 1 would apply whenever $b_{G_{9F}, C} > 0.3323$.

B. Case Study: Poles in RHP

We evaluate the ν -gap metric on a discrete-time SISO case study with sampling time $T_s = 1$ s. Consider the stable plant

$$G_1(z) = \frac{1 - z^{-1}}{1 - 0.8z^{-1}}, \quad G_2(z) = 1.8z^{-1}G_1(z). \quad (11)$$

Plant G_2 differs from G_1 by a gain of 1.8 and an additional one-sample delay z^{-1} , which introduces extra phase lag. We can obtain explicit expressions for the index functions on the unit circle $z = e^{j\omega}$. Since the plants are SISO with real coefficients, $G_1(e^{-j\omega}) = \overline{G_1(e^{j\omega})}$, and thus

$$f_1(e^{j\omega}) = 1 + G_1(e^{j\omega})G_1(e^{-j\omega}) = 1 + |G_1(e^{j\omega})|^2,$$

$$f_2(e^{j\omega}) = 1 + G_2(e^{j\omega})G_1(e^{-j\omega}) = 1 + G_2(e^{j\omega})\overline{G_1(e^{j\omega})}.$$

By (11), we can simplify $f_2(e^{j\omega})$ as

$$f_2(e^{j\omega}) = 1 + 1.8e^{-j\omega}|G_1(e^{j\omega})|^2.$$

Note that $f_1(e^{j\omega})$ is real and strictly positive for all ω , hence $\text{wno}(f_1) = 0$. In contrast, the factor $e^{-j\omega}$ induced by the one-sample delay rotates the complex term in $f_2(e^{j\omega})$ as ω varies, so the curve $f_2(e^{j\omega})$ may encircle the origin, yielding $\text{wno}(f_2) \neq 0$.

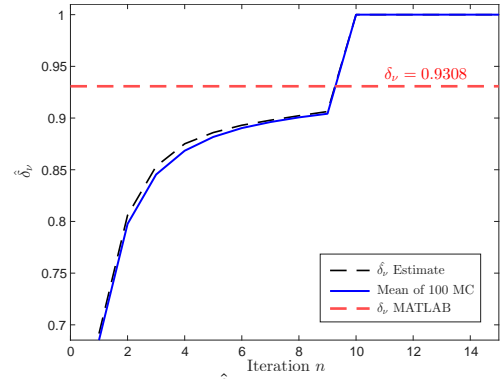


Fig. 4: Estimate of the ν -gap $\hat{\delta}_\nu$ (black, dashed), average of 100 MC simulations (blue, solid), and actual δ_ν (red, dashed).

Using $N_{\text{acc}} = 10$, $N = 1000$, $T_s = 1$, and $\sigma_y^2 = 0.01$, Fig. 4 shows that the power-iteration estimate initially approaches MATLAB’s value $\delta_\nu = 0.9308$. However, at $n = N_{\text{acc}}$, Algorithm 2 detects $\text{wno}(f_1) \neq \text{wno}(f_2)$, so the pair fails the set \mathcal{C} condition. Hence, our procedure applies a hard stop and does not refine the estimate further.

VI. CONCLUSION

We have presented an identification-free, data-driven method to estimate the Vinnicombe ν -gap between two discrete-time SISO systems directly from time-domain input-output experiments. The proposed procedure combines iterative ν -gap estimation with a data-driven admissibility check, providing a control-relevant measure of model mismatch for closed-loop analysis. Numerical studies, including an industrially motivated case, show close agreement with MATLAB’s `gapmetric` and correct detection of index-condition violations. Future work will address extension to MIMO systems.

REFERENCES

- [1] C. A. Desoer and M. Vidyasagar, *Feedback Systems: Input-Output Properties*. SIAM, 2009.
- [2] A. Megretski and A. Rantzer, “System analysis via integral quadratic constraints,” *IEEE Transactions on Automatic Control*, vol. 42, pp. 819–830, 1997.
- [3] K. Zhou, J. C. Doyle, and K. Glover, *Robust and Optimal Control*. Prentice-Hall, 1996.
- [4] G. Vinnicombe, “Structured uncertainty and the graph topology,” in *Proceedings of the 30th IEEE CDC*, pp. 541–542, 1991.
- [5] G. Vinnicombe, “On the frequency response interpretation of an indexed \mathcal{L}_2 -gap metric,” in *American Control Conference*, pp. 1133–1137, 1992.
- [6] A. El-Sakkary, “The gap metric: Robustness of stabilization of feedback systems,” *IEEE Transactions on Automatic Control*, vol. 30, pp. 240–247, 1985.
- [7] M. Cantoni and H. Pfifer, “Gap metric computation for time-varying linear systems on finite horizons,” *IFAC-PapersOnLine*, vol. 50, no. 1, pp. 14513–14518, 2017.
- [8] A. Koch, *Determining input-output properties of linear time-invariant systems from data*. Logos Verlag, 2022.
- [9] T. Koenings, M. Krueger, H. Luo, and S. X. Ding, “A data-driven computation method for the gap metric and the optimal stability margin,” *IEEE Transactions on Automatic Control*, vol. 63, no. 3, pp. 805–810, 2017.
- [10] B. Wahlberg, M. B. Syberg, and H. Hjalmarsson, “Non-parametric methods for \mathcal{L}_2 -gain estimation using iterative experiments,” *Automatica*, vol. 46, no. 8, pp. 1376–1381, 2010.
- [11] C. R. Rojas, T. Oomen, H. Hjalmarsson, and B. Wahlberg, “Analyzing iterations in identification with application to nonparametric \mathcal{H}_∞ -norm estimation,” *Automatica*, vol. 48, no. 11, pp. 2776–2790, 2012.

- [12] M. I. Müller and C. R. Rojas, "Gain estimation of linear dynamical systems using Thompson sampling," in *Proceedings of the 22nd International Conference on Artificial Intelligence and Statistics (AISTATS)*, pp. 1535–1543, 2019.
- [13] M. A. Guerrero, B. Lakshminarayanan, and C. R. Rojas, "Data-driven estimation of structured singular values," *IEEE Control Systems Letters*, vol. 9, pp. 1976–1981, 2025.
- [14] G. H. Golub and C. F. Van Loan, *Matrix Computations*. John Hopkins University Press, 2013.
- [15] K. J. Åström and R. Murray, *Feedback Systems: An Introduction for Scientists and Engineers*. Princeton University Press, 2021.
- [16] P. Welch, "The use of fast Fourier transform for the estimation of power spectra: A method based on time averaging over short, modified periodograms," *IEEE Transactions on Audio and Electroacoustics*, vol. 15, no. 2, pp. 70–73, 1967.
- [17] L. Ljung, *System Identification: Theory for the User, 2nd Edition*. Prentice Hall, 1999.
- [18] W. I. Rowen, "Simplified mathematical representations of heavy-duty gas turbines," *Journal of Engineering for Power*, vol. 105, pp. 865–869, 1983.
- [19] M. R. B. Tavakoli, B. Vahidi, and W. Gawlik, "An educational guide to extract the parameters of heavy duty gas turbines model in dynamic studies based on operational data," *IEEE Transactions on Power Systems*, vol. 24, no. 3, pp. 1366–1374, 2009.
- [20] A. Khormali, I. Yousefi, H. Yahyaei, and S. M. Aliyari, "Identification of an industrial gas turbine based on rowen's model and using multi-objective optimization method," in *3rd RSI ICROM*, pp. 482–487, 2015.
- [21] L. B. Davis and S. Black, "Dry low NO_x combustion systems for GE heavy-duty gas turbines," ASME, 1996.
- [22] K. Venkataraman, S. E. Lewis, J. Natarajan, S. R. Thomas, and J. V. Citenò, "F-class DLN technology advancements: DLN2.6+," in *Turbo Expo: Power for Land, Sea, and Air*, vol. 54631, pp. 587–594, 2011.